

Wavelength selection for quantum cascade lasers by cavity length

Christina Young,^{1,2,a)} Richard Cendejas,¹ Scott S. Howard,^{1,b)}
Wendy Sanchez-Vaynshteyn,^{1,3} Anthony J. Hoffman,¹ Kale J. Franz,¹ Yu Yao,¹
Boris Mizaikoff,^{2,4} Xiaojun Wang,⁵ Jenyu Fan,⁵ and Claire F. Gmachl¹

¹Department of Electrical Engineering, Princeton University, Princeton, New Jersey 08544, USA

²School of Chemistry and Biochemistry, Georgia Institute of Technology, Atlanta, Georgia 30332, USA

³Department of Biomedical Engineering, The City College of New York, New York 10031, USA

⁴Institute of Analytical and Bioanalytical Chemistry, University of Ulm, 89081 Ulm, Germany

⁵Adtech Optics, Inc., City of Industry, California 91748, USA

(Received 26 November 2008; accepted 10 February 2009; published online 4 March 2009)

A systematic shift in spectral emission wavenumbers in quantum cascade lasers (QCLs) is observed over a variation in cavity lengths from 0.5 to 3 mm resulting in a gain peak shift ranging from 2404 to 2286 cm^{-1} . Thereby, a wavelength selection range of 118 cm^{-1} is provided, which is sufficiently broad for selecting the laser emission across the entire CO_2 absorption band at 2326 cm^{-1} (4.3 μm). In contrast to current QCL wavelength selection techniques, modifying the cavity length is a straightforward postprocessing procedure. Experimental evidence confirms that this frequency shift is due to a change in threshold voltage and applied electric field as a function of cavity length which is in agreement with the theory. © 2009 American Institute of Physics.

[DOI: 10.1063/1.3093422]

The ability to deliberately select a quantum cascade laser (QCL) emission frequency is of significant interest for precisely overlapping analyte vibrational-rotational absorption bands with the laser emission, thereby providing inherent molecular selectivity and enhanced sensitivity for trace gas and liquid chemical sensors.^{1,2} Current methods for selecting the QCL emission frequency include the use of an external cavity,^{3–8} an array of single-mode lasers with a variety of emission frequencies monolithically fabricated on one chip,⁹ or adjusting the heatsink temperature using a cryostat or dc laser injection current.^{9–11} External cavity tunable QCLs^{3–8} operate by changing the angle of an external diffraction grating, which creates single mode emission via frequency selective feedback, thereby continuously tuning over a broad spectral range.¹ Although a tuning range of over 250 cm^{-1} has recently been demonstrated,⁸ the gain spectrum does not tune at all or at a much smaller rate than optical tuning, therefore resulting in a decrease in output power for both blueshift and redshift from the central emission. While a shift of the gain spectrum may be achieved by temperature tuning, this is not widely applicable to room temperature operated systems; therefore, alternative strategies for tuning the gain spectrum are in demand.

The present study describes tailoring the QCL cavity length for tuning the gain spectrum. The cavity length is a straightforward postprocessing selection parameter, and therefore ideally suited for conveniently adjusting the QCL gain spectrum and selecting the peak gain wavelength. For the QCL presented here, the wavelength selection range is wide enough to span an entire vibrational-rotational absorption feature of carbon dioxide (CO_2).

Quantum cascade lasers designed for a central emission frequency at 2326 cm^{-1} (4.3 μm) were used. A corresponding band diagram is shown in Fig. 1(a). The layer sequence

in Angstroms of one period of the active region and injector is **26/17/22/18/19/18/21/17/21/15/27/15/38/11/13/36/14/34/14/30/22**, where $\text{Al}_{0.65}\text{In}_{0.35}\text{As}$ barrier layers are marked in bold, $\text{Ga}_{0.32}\text{In}_{0.68}\text{As}$ well layers are given in regular font, and n -doped ($2.1 \times 10^{17} \text{ cm}^{-3}$) layers are underlined. We calculate the conduction band energy diagram of this structure as a function of the applied electric field from 87 to 116 kV/cm yielding an expected transition frequency range from 2137 to 2583 cm^{-1} , as illustrated in Fig. 1(b). The calculated

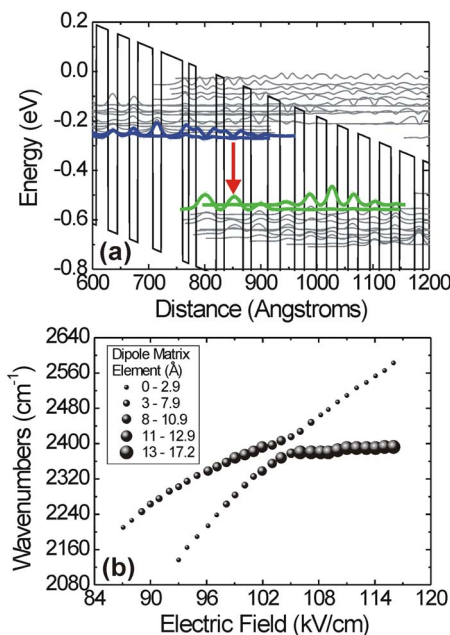


FIG. 1. (Color online) (a) Conduction band energy diagram of the QCL designed to emit at 4.3 μm . (b) Theoretical prediction of the laser emission wavenumber vs electric field. Shown are the peak transition energies for the upper laser level and injector ground level to the lower laser level. The optical dipole matrix element is the strength of the frequency transition, as indicated by the size of the symbols. The overall blueshift of the transition with increasing field can be seen.

^{a)}Electronic mail: christina.young@chemistry.gatech.edu.

^{b)}Present address: Cornell University, Department of Applied and Engineering Physics, Ithaca, NY 14850.

frequency increases with increasing applied electric field due to the linear Stark effect inherent to the “diagonal” transition design.¹² The dipole matrix element indicates the strength of the optical transition, and is at maximum around the designated electric field of 103 kV/cm, which coincides with the anticrossing field. As the emission frequency depends on the operating threshold voltage [Fig. 1(b)], a change in laser threshold voltage enables tuning of the gain spectrum. The former can be achieved by changing the threshold current density, which in turn is most efficiently modified by changing the cavity length.

To analyze cavity length effects, the QCLs were cleaved at lengths ranging from 0.5 to 3 mm in increments of 0.5 mm using a diamond knife and microscopic control. Laser ridge widths ranged from 4.6 to 6.1 μm . Each laser was then mounted using indium onto a copper block, which served as both a heatsink and an electrical ground, and then bonded with gold wires.

The QCLs were operated in pulsed mode using a pulse generator with a frequency of 80 kHz, and a pulse width of 100 ns. Bias was applied to each QCL and was independently measured, while current was simultaneously measured using a current probe. Heatsink temperatures varied between 80 and 300 K. The spectra were then acquired using a liquid nitrogen cooled mercury-cadmium-telluride detector, and a Fourier-transform infrared (FTIR) spectrometer at a spectral resolution of 0.125 cm^{-1} , and by averaging ten scans. Figure 2(a) depicts FTIR measured peak emission spectra as wavenumber versus heatsink temperature ranging from 80 to 300 K for various cavity lengths. The emission frequency decreases from 2404 to 2286 cm^{-1} , i.e., by 118 cm^{-1} , with an increase in cavity length from 0.5 to 3 mm. A carbon dioxide (CO_2) FTIR absorbance spectrum is provided in Fig. 2(a). Evidently, QCLs with cavity lengths of 1.5, 2, and 3 mm directly overlap with strong vibrational-rotational absorption bands at various temperatures. Similarly, different cavity lengths can be used to deliberately overlap or to avoid overlapping with selected CO_2 features, as shown in Fig. 2(b). It is shown that at constant heatsink temperature cavity lengths in the range of 1–2 mm, span across the entire absorption spectrum. Thus, a convenient postprocessing strategy for tailoring on- and off-resonance QCLs is provided, whereby a differential measurement directly yields a quantitative determination of the analyte concentration. Figure 2(c) describes the relationship of the emission frequency with the cavity length across a range of heatsink temperatures. The data in this figure further clarifies the ability to systematically select emission frequencies using a range of different cavity lengths.

Lasers with a length of 0.5, 1, and 1.5 mm in Fig. 2 did not fully lase to room temperature due to the higher threshold current density (determined by mirror loss) exceeding the maximum available current density (determined by the doping density). To overcome this limitation, and also to shift emission frequency to directly overlap CO_2 absorption features at higher operating temperatures, the 1 and 1.5 mm lasers described in Fig. 3 were prepared with a high reflection (HR) coating. It should be noted that HR coating lasers change the mirror losses from those expected for a standard laser of that length and thus result in a shift in wavelength. However, dependence of the cavity length on the threshold voltage is still clearly evident in the results presented herein,

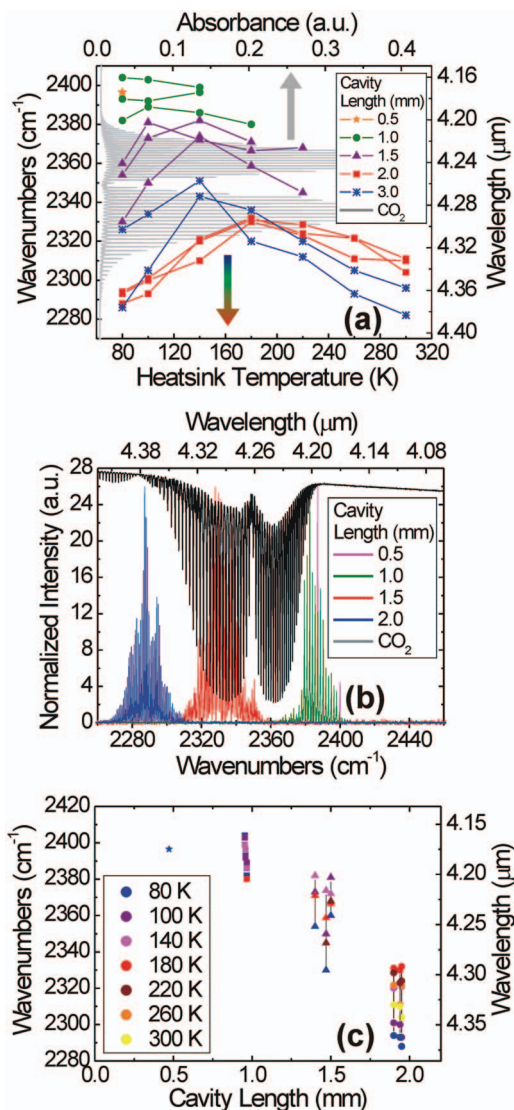


FIG. 2. (Color) (a) Measured emission wavenumber as a function of the heatsink temperature and QCL cavity length. (b) QCL emission spectra of four different cavity lengths on and off resonance with carbon dioxide. All spectra were taken at 80 K. (c) Emission wavenumber as a function of the QCL cavity length and heatsink temperature.

which is in turn itself responsible for a corresponding shift in emission wavenumbers.

Temperature dependent light-current-voltage (L - I - V) measurements were performed using 100 ns current pulses at a repetition rate of 3 kHz to precisely determine the threshold voltage and the threshold current density. Figure 3(a) represents the relationship between threshold voltage and wavenumbers. From this figure, it is confirmed that the threshold voltage and the spectral emission increase with decreasing cavity length. These experimental results substantiate the calculations provided in Fig. 1(b), which suggest an increase in spectral emission energy with an increasing applied electric field. It should be noted however that the calculations of the Stark effect in QCLs using the full states [see Fig. 1(a)] usually overestimate the Stark shift, as was also discussed in Ref. 12.

Figure 3(b) demonstrates the dependence of the threshold voltage on 1, 1.5, and 2 mm cavity lengths over heatsink temperatures ranging from 80 to 180 K. In this graph, it is further shown that shorter cavity lengths have a higher

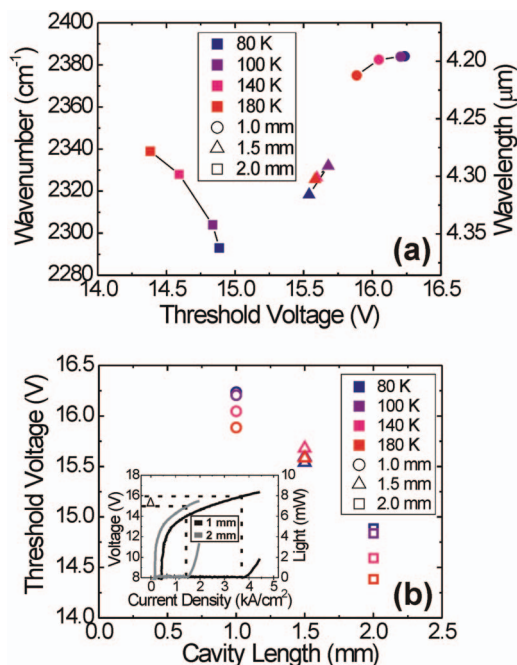


FIG. 3. (Color) (a) Measured emission frequency as a function of threshold voltage for cavity lengths of 1, 1.5, and 2 mm. (b) Threshold voltage as a function of cavity length and heatsink temperature. Inset: $L-I-V$ characteristics of QCLs with 1 mm (black) and 2 mm (gray) cavity lengths.

threshold voltage than longer cavity lengths due to their higher threshold current densities. Figure 3(b) (inset) quantifies this trend with an $(L-I-V)$ plot where threshold voltages are measured as 16.2 and 14.9 V, and threshold current densities as 4.17 and 1.39 kA/cm^2 for 1 and 2 mm cavity lengths, respectively. The difference in threshold voltages as a function of cavity length was calculated to be 1.35 V. Thus, threshold voltages increase with a decrease in cavity length, which consequently results in higher spectral emission frequency due to the increase in electric field.

In summary, this inexpensive and straightforward QCL wavelength selection technique takes advantage of the elec-

tric field and spectral emission dependence on the cavity length, which is considered a simple postprocessing device parameter. Consequently, the same wafer and the same chip may simply be cleaved to produce a desired emission frequency with high specificity and reproducibility. Varying the cavity length from 0.5 to 3 mm provides a wide selection range of 118 cm^{-1} , which is broad enough to tailor on and off resonances across the entire CO_2 vibrational-rotational absorption bands at $4.3 \mu\text{m}$ without temperature tuning. Therefore, the proposed strategy appears particularly useful for tailoring the laser emission frequency in chemical sensor applications.

The authors would like to acknowledge support from MIRTHERC, NSF-REU, and ExxonMobil Research and Engineering Co. Fruitful discussions with Fatima Toor and Afusat Dirisu are gratefully acknowledged.

- ¹C. Young, S.-S. Kim, and B. Mizaikoff, in *Lasers in Chemistry*, edited by M. Lackner (Wiley, Weinheim, 2008).
- ²C. Young, S.-S. Kim, Y. Luzinova, M. Weida, D. Arnone, E. Takeuchi, T. Day, and B. Mizaikoff, *Sens. Actuators B* (in press).
- ³G. P. Luo, C. Peng, H. Q. Le, S. S. Pei, W.-Y. Hwang, B. Ishaug, J. Um, J. N. Baillargeon, C.-H. Lin, and A. Y. Cho, *Appl. Phys. Lett.* **78**, 2834 (2001).
- ⁴C. Peng, G. Luo, and H. Q. Le, *Appl. Opt.* **42**, 4877 (2003).
- ⁵R. Maulini, M. Beck, J. Faist, and E. Gini, *Appl. Phys. Lett.* **84**, 1659 (2004).
- ⁶G. Wysocki, R. F. Curl, F. K. Tittel, F. Capasso, L. Diehl, M. Troccoli, G. Höfler, R. Maulini, and J. Faist, *Appl. Phys. B: Lasers Opt.* **81**, 769 (2005).
- ⁷H. L. Zhang, C. Peng, A. Seetharaman, G. P. Luo, Q. Le Han, C. Gmachl, D. L. Sivco, and A. Y. Cho, *Appl. Phys. Lett.* **86**, 111112 (2005).
- ⁸R. Maulini, A. Mohan, M. Giovannini, J. Faist, and E. Gini, *Appl. Phys. Lett.* **88**, 201113 (2006).
- ⁹B. G. Lee, M. A. Belkin, R. Audet, J. MacArthur, L. Diehl, C. Pflügl, F. Capasso, D. C. Oakley, D. Chapman, A. Napoleone, D. Bour, S. Corzine, and G. Höfler, *Appl. Phys. Lett.* **91**, 231101 (2007).
- ¹⁰J. Faist, C. Gmachl, F. Capasso, C. Sirtori, D. L. Sivco, J. N. Baillargeon, and A. Y. Cho, *Appl. Phys. Lett.* **70**, 2670 (1997).
- ¹¹A. Müller, M. Beck, and J. Faist, *Appl. Phys. Lett.* **75**, 1509 (1999).
- ¹²Y. Yao, Z. Liu, A. J. Hoffman, K. J. Franz, and C. F. Gmachl, *IEEE J. Quantum Electron.* (in press).